





## Symmetry energy dilemma within a relativistic quark model

Himanshu S. Sahoo <sup>1</sup>, Supriya Karan <sup>2</sup>, Rabindranath Mishra <sup>1</sup> and Prafulla K. Panda <sup>2</sup>

<sup>1</sup>*Department of Physics, Ravenshaw University, Cuttack-753 003, India*

<sup>2</sup>*Department of Physics, Utkal University, Bhubaneswar-751 004, India*



(Received 20 August 2021; accepted 15 November 2021; published 23 November 2021)

We develop the equation of state of dense neutron star matter with nucleons, nucleons and hyperons, nucleons and delta, as well as including strange interactions through strange meson-hyperon couplings to assess the effect of both the soft and stiff symmetry energy, determined in the recent PREX-II experiment, on the properties of neutron stars. The macroscopic properties of neutron stars such as the mass, radius and tidal deformability are a direct consequence of the underlying equation of state of dense neutron star matter. Given the recent advances in constraining the above macroscopic observations from gravitational wave analysis, NICER and radio observations, we study here the effect of a variation in the symmetry energy on such observational properties of neutron stars with different possible compositions in a relativistic quark model. We observe that the stiff symmetry energy satisfies the current constraints on maximum mass and radius, but creates tension with tidal deformability values.

DOI: [10.1103/PhysRevC.104.055805](https://doi.org/10.1103/PhysRevC.104.055805)

### I. INTRODUCTION

Recent developments in the field of nuclear astrophysics and gravitational wave astronomy have provided novel data on neutron star masses, radii, and tidal deformabilities. Concurrent developments in terrestrial nuclear experiments such as the measurement of neutron skin of  $^{108}\text{Pb}$  by the PREX-II collaboration [1] with a precision of nearly 1% have also contributed exciting data on the possible values of nuclear symmetry energy ( $J$ ) around the nuclear saturation density. These results have no doubt significantly enhanced our understanding of dense matter physics and structure of neutron stars and yet at the same time have provided new challenges [2] to our current understanding of density dependence of nuclear symmetry energy.

The accepted values of the symmetry energy currently used in the literature have been determined from various [3–9] theoretical as well as experimental analyses. The fiducial value of  $J$  from a survey of 29 analyses [10] was determined to  $J = 31.6 \pm 2.7$  MeV with the corresponding slope parameter  $L = 58.9 \pm 16$  MeV. It was then revised to  $J = 31.7 \pm 3.2$  and  $L = 58.7 \pm 28.1$  MeV from a study of 53 analyses [11]. A recent study based on the Bayesian analysis of chiral effective field theory predictions [5] suggested the values of  $J = 31.7 \pm 1.1$  MeV and  $L = 59.8 \pm 4.1$  MeV.

While the fiducial values of the symmetry energy from the above studies is more or less the same as those obtained from the analyses of neutron star observational data post-GW170817 [12], the values for  $L$  and the curvature parameter  $K_{\text{sym}}^0$  have been newly extracted [12]. The mean value of  $L$  at a 68% confidence level from 24 new analyses has been determined to  $L \approx 57.7 \pm 19$  MeV and the mean value of  $K_{\text{sym}}^0$  at a 68% confidence level from 16 new analyses has been determined to  $K_{\text{sym}}^0 \approx -107 \pm 88$ .

Recent terrestrial nuclear experiments are however signaling higher ranges for the above. The recent measurement [13] of spectra of charged pions produced by colliding rare isotope tin (Sn) beams with isotopically enriched tin targets suggests the slope of the symmetry energy to be  $42 < L < 117$  MeV. Even more intriguing is the result from the updated Lead Radius EXperiment (PREX-II) [1] which has determined the neutron skin thickness of  $^{108}\text{Pb}$  to  $R_{\text{skin}} = (0.283 \pm 0.071)$  fm, suggesting the limits [2] of  $\mathcal{E}_{\text{sym}} = (38.1 \pm 4.7)$  MeV and  $L = (106 \pm 37)$  MeV. These limits are considerably greater than those obtained from the modeling of astrophysical data and predict a stiff symmetry energy around saturation density, which is contrary to accepted norms.

Since the symmetry energy plays a significant role in constraining neutron star properties like the stellar radii, we attempt here to analyze the impact of the above-discussed contrasting values of  $J$  (termed a “dilemma” by Piekarewicz [14]) on the structure and properties of neutron stars. Several attempts have been made to analyze the above properties using relativistic mean-field (RMF) models. It is worth mentioning here that RMF models consider nucleons as structureless point objects. These models realize the nucleon-nucleon interactions through the coupling of nucleons with  $\sigma$ ,  $\omega$ , and  $\rho$  mesons and their self- and crossed interactions besides photons and explain well the observed bulk properties of nuclear matter including the nuclear equation of state (EoS) and also various properties of finite nuclei. However, incorporation of structure of nucleon with meson couplings at the basic quark level in the study of saturation properties of nuclear matter can provide new insight [15,16]. It gave birth to quark-meson-coupling (QMC) models. In the QMC model, nuclear matter is described as a system of nonoverlapping MIT bags which interact through the effective scalar and vector mean fields, very much in the same way as in the Walecka model. Saito,

Thomas, and their collaborators [17,18] and others [19,20] have very successfully studied various properties of nuclear matter on the basis of QMC models. Significant studies [21–24] on the structure and composition of neutron stars have also been made using the QMC model. There have also been several attempts to study neutron star matter by describing the structure of nucleons through a relativistic quark model (RQM) in conjunction with the RMF model.

We therefore applied a relativistic quark model alternatively called the modified quark meson coupling model (MQMC) [25–29] to develop the EoS of dense neutron star matter. Unlike the QMC model [15], it uses an equal mixture of scalar and vector harmonic potential to confine the relativistic independent quarks to realize the structure of hadron in vacuum. Here we study the effect of variation in  $J$  on the observational properties of neutron stars with nonstrange as well as strange hadronic composition. The results so obtained are compared with the recent multimessenger observations post GW170817 event [30–33] as well as the results from the simultaneous mass-radius measurement of PSR J0030+0451 [34,35] and radius measurement of PSR J0740+6620 by the NICER collaboration [36,37]. We also study the variation of the speed of sound and the adiabatic index with different compositions of matter.

The paper is organized as follows: In Sec. II, a brief formalism of the model describing the baryon structure in vacuum is discussed and the EoS is developed. In Sec. III the EoS for the symmetric as well as neutron star matter is developed while we discuss the results in Sec. IV.

## II. MODIFIED QUARK MESON COUPLING MODEL

The modified quark-meson-coupling model has been widely applied for the study of the bulk properties of symmetric and asymmetric nuclear matter [25–29,38–40] including hyperons, delta isobars, as well as strange interactions. In such a model the baryons are described as being composed of three constituent quarks in a phenomenological flavor-independent confining potential,  $U(r)$  in an equally mixed scalar and vector harmonic form inside the baryon [25], where

$$U(r) = \frac{1}{2}(1 + \gamma^0)V(r),$$

with

$$V(r) = (ar^2 + V_0), \quad a > 0. \quad (1)$$

Here  $(a, V_0)$  are the potential parameters. The confining interaction provides the zeroth-order quark dynamics of the hadron. In the medium, the quark field  $\psi_q(\mathbf{r})$  satisfies the Dirac equation

$$\begin{aligned} & [\gamma^0 (\epsilon_q - V_\omega - \frac{1}{2}\tau_{3q}V_\rho - V_\phi) - \vec{\gamma} \cdot \vec{p} \\ & - (m_q - V_\sigma - V_{\sigma^*}) - U(r)] \psi_q(\vec{r}) = 0, \end{aligned} \quad (2)$$

where  $V_\sigma = g_\sigma^q \sigma_0$ ,  $V_\omega = g_\omega^q \omega_0$ ,  $V_\rho = g_\rho^q b_{03}$ ,  $V_\phi = g_\phi^q \phi_0$ , and  $V_{\sigma^*} = g_{\sigma^*}^q \sigma_0^*$ . Here  $\sigma_0$ ,  $\omega_0$ ,  $b_{03}$ ,  $\sigma_0^*$ , and  $\phi_0$  are the classical meson fields;  $g_\sigma^q$ ,  $g_\omega^q$ ,  $g_\rho^q$ ,  $g_{\sigma^*}^q$ , and  $g_\phi^q$  are the quark couplings to the  $\sigma$ ,  $\omega$ ,  $\rho$ ,  $\sigma^*$ , and  $\phi$  mesons, respectively;  $m_q$  is the quark mass; and  $\tau_{3q}$  is the third component of the Pauli matrices. We

can now define

$$\epsilon'_q = (\epsilon_q^* - V_0/2) \quad \text{and} \quad m'_q = (m_q^* + V_0/2), \quad (3)$$

where the effective quark energy  $\epsilon_q^* = \epsilon_q - V_\omega - \frac{1}{2}\tau_{3q}V_\rho - V_\phi$  and effective quark mass  $m_q^* = m_q - V_\sigma - V_{\sigma^*}$ . We now introduce  $\lambda_q$  and  $r_{0q}$  as

$$(\epsilon'_q + m'_q) = \lambda_q \quad \text{and} \quad r_{0q} = (a\lambda_q)^{-\frac{1}{4}}. \quad (4)$$

The ground-state quark energy can be obtained from the eigenvalue condition

$$(\epsilon'_q - m'_q) \sqrt{\frac{\lambda_q}{a}} = 3. \quad (5)$$

The solution of Eq. (5) for the quark energy  $\epsilon_q^*$  immediately leads to the mass of baryon in the medium in zeroth order as

$$E_B^{*0} = \sum_q \epsilon_q^*. \quad (6)$$

Corrections due to spurious center-of-mass motion,  $\epsilon_{\text{c.m.}}$ , as well as those due to other residual interactions, such as the one-gluon exchange at short distances  $(\Delta E_B)_g$ , and quark-pion coupling arising out of chiral symmetry restoration  $\delta M_B^\pi$ , have been considered in a perturbative manner, described explicitly in Refs. [25,27], to obtain the effective baryon mass.

Treating these energy corrections independently, the effective mass of the baryon in the medium becomes

$$M_B^*(\sigma, \sigma^*) = E_B^{*0} - \epsilon_{\text{c.m.}} + \delta M_B^\pi + (\Delta E_B)_g^E + (\Delta E_B)_g^M. \quad (7)$$

Once the effective mass of the baryon is realized, it is used within a relativistic mean-field formalism [25–29] to determine the EoS for asymmetric nuclear matter as well as neutron star matter under different compositions and interactions. This is briefly reviewed in the following sections.

## III. THE EQUATION OF STATE

### A. The EoS for nuclear matter and the symmetry energy

At a specific baryon density, the total energy density and pressure of nuclear matter is given by

$$\mathcal{E} = \frac{1}{2}m_\sigma^2\sigma_0^2 + \frac{1}{2}m_\omega^2\omega_0^2 + \frac{1}{2}m_\rho^2b_{03}^2 \quad (8)$$

$$+ \frac{\gamma}{(2\pi)^3} \sum_{N=p,n} \int^{k_{f,N}} d^3k \sqrt{k^2 + M_N^{*2}}, \quad (9)$$

$$P = -\frac{1}{2}m_\sigma^2\sigma_0^2 + \frac{1}{2}m_\omega^2\omega_0^2 + \frac{1}{2}m_\rho^2b_{03}^2 \quad (10)$$

$$+ \frac{\gamma}{3(2\pi)^3} \sum_{N=p,n} \int^{k_{f,N}} \frac{k^2 d^3k}{\sqrt{k^2 + M_N^{*2}}}, \quad (11)$$

where  $\gamma = 2$  is the spin degeneracy factor for nuclear matter. The nucleon density becomes

$$\rho_N = \frac{\gamma}{(2\pi)^3} \int_0^{k_{f,N}} d^3k = \frac{\gamma k_{f,N}^3}{6\pi^2} \quad \text{where } N = p, n. \quad (12)$$

Therefore, the total baryon density becomes  $\rho_B = \rho_p + \rho_n$  and the (third component of) isospin density  $\rho_3 = \rho_p - \rho_n$ .

The vector mean fields  $\omega_0$  and  $b_{03}$  are determined through

$$\omega_0 = \frac{g_\omega}{m_\omega^2} \rho_B \quad b_{03} = \frac{g_\rho}{2m_\rho^2} \rho_3, \quad (13)$$

where  $g_\omega = 3g_\omega^q$  and  $g_\rho = g_\rho^q$ . Fixing the scalar mean field  $\sigma_0$  as

$$\frac{\partial \mathcal{E}}{\partial \sigma_0} = 0. \quad (14)$$

The isoscalar scalar and isoscalar vector couplings  $g_\sigma^q$  and  $g_\omega$  are fit to the saturation density and binding energy for nuclear matter while the isovector vector coupling  $g_\rho$  is fixed using symmetry energy;  $\omega_0$ ,  $b_{03}$ , and  $\sigma_0$  are determined from Eqs. (13) and (14), respectively.

The nuclear symmetry energy describes the increase in the energy of nuclear matter with the increase in isospin asymmetry. It can be defined as the difference between the total energy per baryon  $\mathcal{E}/\rho_B$  of pure neutron matter and that of isospin-symmetric matter at baryon density  $\rho_B$ . It can be expressed as [26]

$$\mathcal{E}_{\text{sym}}(\rho_B) = \frac{k_{f,N}^2}{6E_{f,N}^*} + \frac{g_\rho^2}{8m_\rho^2} \rho_B, \quad (15)$$

where  $E_{f,N}^* = (k_{f,N}^2 + M_N^{*2})^{1/2}$ .

For nuclear matter at densities in excess of the saturation density  $\rho_0$ , we may define the symmetry energy parameters as

$$\begin{aligned} J &= \mathcal{E}_{\text{sym}}(\rho_0) \\ L &= 3\rho_0 \left. \frac{\partial \mathcal{E}_{\text{sym}}(\rho_B)}{\partial \rho_B} \right|_{\rho_B=\rho_0} \quad (\text{slope of } \mathcal{E}_{\text{sym}}) \\ K_{\text{sym}}^0 &= 9\rho_0^2 \left. \frac{\partial^2 \mathcal{E}_{\text{sym}}(\rho_B)}{\partial \rho_B^2} \right|_{\rho_B=\rho_0} \quad (\text{curvature of } \mathcal{E}_{\text{sym}}). \end{aligned} \quad (16)$$

### B. The EoS of neutron star matter

In the present work, we have considered four different compositions of neutron star matter, namely matter consisting only of nucleons ( $N =$  neutrons and protons), matter

TABLE I. The slope and curvature parameter of symmetry energy.

$J$ (MeV)	$g_\rho$	$L$ (MeV)	$K_{\text{sym}}^0$ (MeV)	$J(2\rho_0)$ (MeV)
28.5	7.86543	76.2	-23.8	53.2
31.7	8.66225	86.0	-23.8	59.7
34.9	9.39170	95.8	-23.8	66.2
38.1	10.06845	105.6	-23.8	72.8

composed of the baryon octet ( $B = N, \Lambda, \Sigma^\pm, \Sigma^0, \Xi^-, \Xi^0$ ) [27], matter composed of nucleons and the delta isobars ( $\Delta^-, \Delta^0, \Delta^+, \Delta^{++}$ ) [28], and matter involving both nonstrange as well as strange interactions [29] where a pair of hidden strange mesons  $\sigma^*$  and  $\phi$  couple only to the strange quark and hyperons of nuclear matter. We give here a general formalism for obtaining the EoS, while the specific parameters are described under Results and Discussions.

To describe the properties of the core of a neutron star, we extend the usual Lagrangian density in relativistic mean-field approximation to include not only the  $\sigma$ ,  $\omega$ , and  $\rho$  mesons but also the strange mesons, namely the isoscalar, scalar ( $\sigma^*$ ), and vector ( $\phi$ ) mesons. The Lagrangian density is defined as

$$\begin{aligned} \mathcal{L} &= \sum_B \bar{\psi}_B [i\gamma^\mu \partial_\mu - M_B^*(\sigma, \sigma^*) - g_{\omega B} \gamma^\mu \omega_\mu \\ &\quad - g_{\phi B} \gamma^\mu \phi_\mu - g_{\rho B} \gamma^\mu \vec{\rho}_\mu \cdot \vec{I}_B] \psi_B \\ &\quad + \frac{1}{2} (\partial_\mu \sigma \partial^\mu \sigma - m_\sigma^2 \sigma^2) + \frac{1}{2} (\partial_\mu \sigma^* \partial^\mu \sigma^* - m_{\sigma^*}^2 \sigma^{*2}) \\ &\quad + \frac{1}{2} m_\omega^2 \omega_\mu \omega^\mu - \frac{1}{4} \Omega_{\mu\nu} \Omega^{\mu\nu} + \frac{1}{2} m_\phi^2 \phi_\mu \phi^\mu - \frac{1}{4} \Phi_{\mu\nu} \Phi^{\mu\nu} \\ &\quad + \frac{1}{2} m_\rho^2 \vec{b}_\mu \cdot \vec{b}^\mu - \frac{1}{4} \vec{B}_{\mu\nu} \cdot \vec{B}^{\mu\nu} \\ &\quad + \sum_l \bar{\psi}_l [i\gamma^\mu \partial_\mu - m_l] \psi_l, \end{aligned} \quad (17)$$

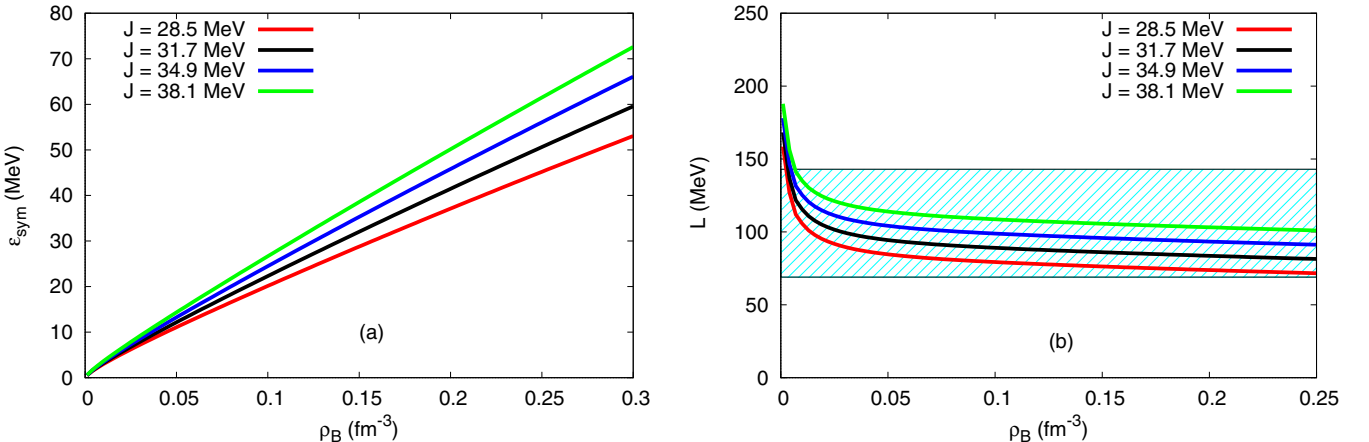


FIG. 1. (a) Symmetry energy as a function of density for four different  $J$  values and (b) the corresponding slope  $L$ . The shaded region shows the range of  $L = 106 \pm 37$  suggested in Ref. [2].

TABLE II. Mass, radius, and dimensionless tidal deformability  $\Lambda_D$  for nucleonic composition of stellar matter. Also shown is the radius  $R_{1.4}$  corresponding to the canonical mass  $1.4 M_\odot$ .

$J$ (MeV)	$M$ ( $M_\odot$ )	$R$ (km)	$R_{1.4}$ (km)	$\Lambda_{D1.4}$
28.5	2.10	11.6	13.6	536
31.7	2.11	11.7	13.7	603
34.9	2.12	11.8	13.9	619
38.1	2.12	11.9	14.1	641

where

$$\begin{aligned}\Omega_{\mu\nu} &= \partial_\mu\omega_\nu - \partial_\nu\omega_\mu, & \Phi_{\mu\nu} &= \partial_\mu\phi_\nu - \partial_\nu\phi_\mu, \\ \vec{B}_{\mu\nu} &= \partial_\mu\vec{b}_\nu - \partial_\nu\vec{b}_\mu\end{aligned}\quad (18)$$

with  $\psi_{B(l)}$  the baryon (lepton) field and  $\vec{I}_B$  the isospin matrix for baryon and  $m_l$  the lepton mass. The hadronic matter is described using a mean-field approach in which the meson fields are treated as classical fields and the field operators are replaced by their expectation values. A detailed description can be found in Ref. [29].

The total energy density ( $\mathcal{E}$ ) and pressure ( $P$ ) at a particular baryon density for the nuclear matter in  $\beta$  equilibrium, consisting of the baryon octet and the leptons  $l = e, \mu$  can be found as

$$\begin{aligned}\mathcal{E} &= \frac{1}{2}m_\sigma^2\sigma_0^2 + \frac{1}{2}m_{\sigma^*}^2\sigma_0^{*2} + \frac{1}{2}m_\omega^2\omega_0^2 + \frac{1}{2}m_\phi^2\phi_0^2 \\ &+ \frac{1}{2}m_\rho^2b_{03}^2 + \frac{\gamma}{2\pi^2} \sum_B \int_0^{k_B} k^2 dk \sqrt{k^2 + M_B^{*2}} \\ &+ \sum_l \frac{1}{\pi^2} \int_0^{k_l} k^2 dk \sqrt{k^2 + m_l^2},\end{aligned}\quad (19)$$

$$\begin{aligned}P &= -\frac{1}{2}m_\sigma^2\sigma_0^2 - \frac{1}{2}m_{\sigma^*}^2\sigma_0^{*2} + \frac{1}{2}m_\omega^2\omega_0^2 + \frac{1}{2}m_\phi^2\phi_0^2 \\ &+ \frac{1}{2}m_\rho^2b_{03}^2 + \frac{\gamma}{6\pi^2} \sum_B \int_0^{k_B} \frac{k^4 dk}{\sqrt{k^2 + M_B^{*2}}} \\ &+ \frac{1}{3} \sum_l \frac{1}{\pi^2} \int_0^{k_l} \frac{k^4 dk}{[k^2 + m_l^2]^{1/2}}.\end{aligned}\quad (20)$$

The composition of neutron star matter with strongly interacting baryons is determined by the requirements of charge neutrality and  $\beta$ -equilibrium conditions under the weak processes. The charge neutrality condition after deleptonization

TABLE III. Mass, radius, and dimensionless tidal deformability  $\Lambda_D$  for stellar matter including nucleons and hyperons.

$J$ (MeV)	$M$ ( $M_\odot$ )	$R$ (km)	$R_{1.4}$ (km)	$\Lambda_{D1.4}$
28.5	1.93	12.4	13.6	529
31.7	1.93	12.5	13.7	598
34.9	1.93	12.7	13.9	621
38.1	1.93	12.8	14.1	654

TABLE IV. Mass, radius, and dimensionless tidal deformability  $\Lambda_D$  for stellar matter including nucleons and Delta isobars.

$J$ (MeV)	$M$ ( $M_\odot$ )	$R$ (km)	$R_{1.4}$ (km)	$\Lambda_{D1.4}$
28.5	1.95	11.9	13.6	534
31.7	1.98	12.1	13.7	590
34.9	2.00	12.2	13.9	618
38.1	2.02	12.4	14.1	632

is given by

$$q_{\text{tot}} = \sum_B q_B \frac{\gamma k_B^3}{6\pi^2} + \sum_{l=e,\mu} q_l \frac{k_l^3}{3\pi^2} = 0, \quad (21)$$

where  $q_B$  corresponds to the electric charge of baryon species  $B$  and  $q_l$  corresponds to the electric charge of lepton species  $l$ . The net strangeness is determined by the condition of  $\beta$  equilibrium which for baryon  $B$  is given by  $\mu_B = b_B\mu_n - q_B\mu_e$ , where  $\mu_B$  is the chemical potential of baryon  $B$  and  $b_B$  its baryon number and  $q_B$  is the charge of the baryon under consideration. Thus the chemical potential of any baryon can be obtained [41] from the two independent chemical potentials  $\mu_n$  and  $\mu_e$  of neutron and electron, respectively.

The relation between the mass and radius of a star with its central density can be determined by integrating the Tolman-Oppenheimer-Volkoff (TOV) equations [42–44] given by

$$\frac{dP}{dr} = -\frac{G(mc^2 + 4\pi r^3 p)(\mathcal{E} + P)}{rc^4(r - 2Gm/c^2)} \quad (22)$$

$$\frac{dm}{dr} = 4\pi r^2 \frac{\mathcal{E}}{c^2}, \quad (23)$$

where  $G$  is the gravitational constant,  $c$  is the speed of light, and  $m$  represents the mass interior to the radius  $r$ . It may be noted here that to describe the crust of the star where the density is significantly smaller than nuclear matter saturation density, we add the standard Baym-Pethick-Sutherland (BPS) EoS [45] to the EoS of the MQMC model.

## IV. RESULTS AND DISCUSSION

### A. Symmetric nuclear matter

The two potential parameters in the MQMC model are obtained by fitting the nucleon mass  $M_N = 939$  MeV and charge radius [46] of the proton ( $r_N$ ) = 0.84 fm in free space. Taking the  $u$  and  $d$  quark mass at  $m_q = 200$  MeV

TABLE V. Mass, radius, and dimensionless tidal deformability  $\Lambda_D$  for stellar matter including nucleons and hyperons with strange interactions.

$J$ (MeV)	$M$ ( $M_\odot$ )	$R$ (km)	$R_{1.4}$ (km)	$\Lambda_{D1.4}$
28.5	2.03	12.2	13.9	584
31.7	2.04	12.3	14.1	638
34.9	2.04	12.4	14.3	730
38.1	2.05	12.5	14.5	699

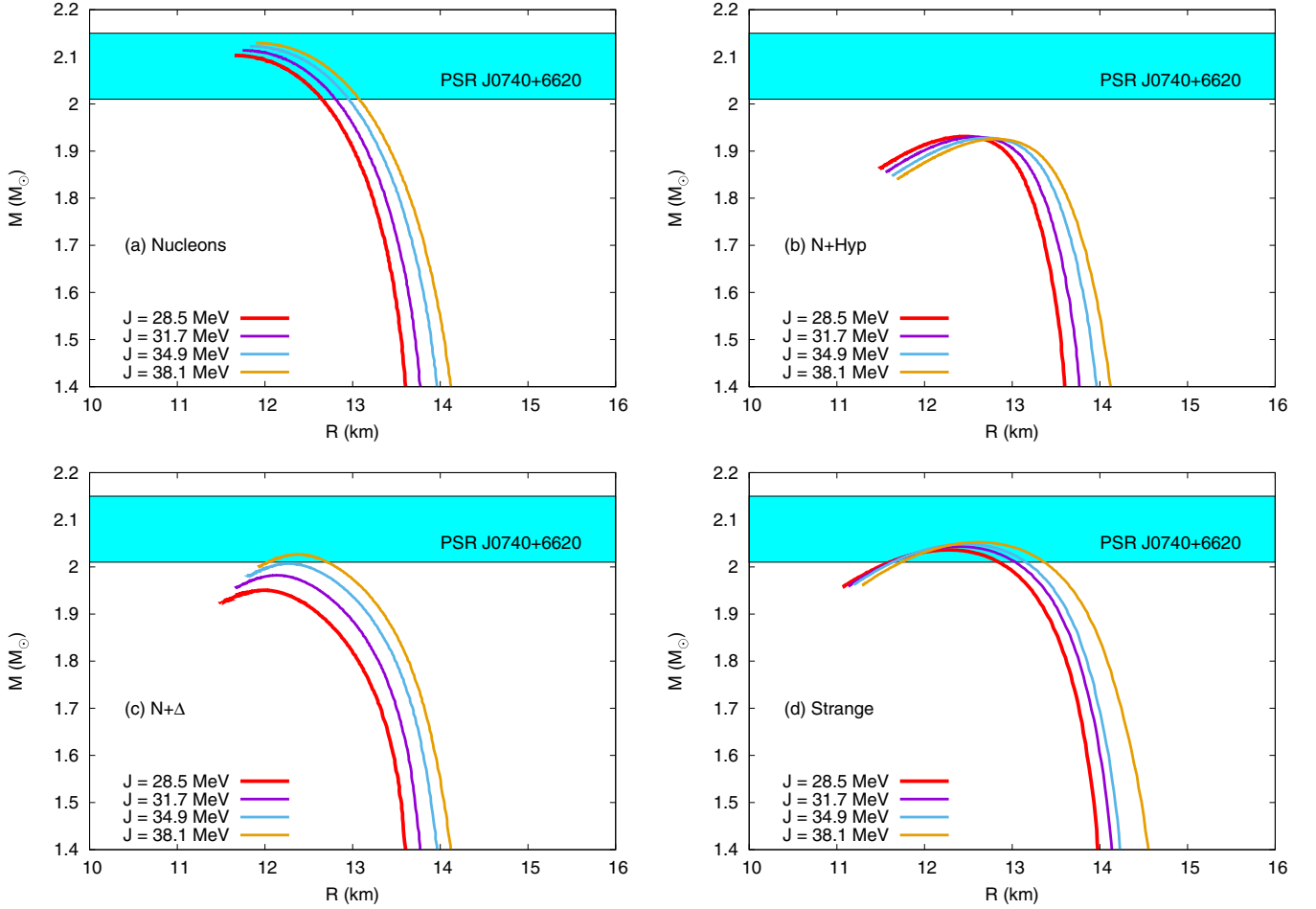


FIG. 2. Neutron star masses as a function of the radius computed for different compositions. Each figure shows the effect of the variation in the  $J$  and the shaded region shows the mass range  $2.08 \pm 0.07 M_{\odot}$  of the pulsar PSR J0740+6620 determined from NICER observations.

along with the standard values for the meson masses (namely  $m_{\sigma} = 550$  MeV,  $m_{\omega} = 783$  MeV, and  $m_{\rho} = 763$  MeV) and fitting the quark-meson coupling constants self-consistently, we obtain the saturation properties of nuclear matter binding energy by setting  $E_{B.E.} \equiv B_0 = \mathcal{E}/\rho_B - M_N = -15.7$  MeV, pressure,  $P = 0$  at  $\rho_B = \rho_0 = 0.15 \text{ fm}^{-3}$ , with the values of  $g_{\sigma}^q = 4.36839$  and  $g_{\omega} = 7.40592$ . The coupling constant  $g_{\rho}$  is fixed for four different values of the symmetry energy. These values are chosen to cover the limits of the current accepted [11] range  $J = 31.7 \pm 3.2$  MeV as well as the significantly stiffer range of  $J = 38.1 \pm 4.7$  MeV. The values of  $g_{\rho}$ , slope of the symmetry energy  $L$ , and the curvature parameter  $K_{\text{sym}}^0$  at saturation density are given in Table I.

The slope of the symmetry energy  $L$  at saturation density increases with increasing  $J$ . For  $J$  values within the limits of  $31.7 \pm 3.2$  MeV, we obtain  $76.2 \leq L \leq 95.8$  MeV and for a stiffer  $J = 38.1$  MeV we get  $L = 105.6$  MeV. Recent studies based on the PREX-II results [2] and the strong correlation between the  $L$  and neutron skin thickness of  $^{208}\text{Pb}$  suggest  $L = (106 \pm 37)$  MeV. More recently, a study [47] based on Bayesian analysis of PREX-II data and GW170817 and NICER observations suggests a range of  $L = 69_{-19}^{+21}$  MeV.

Our results for  $L$  at different  $J$  are consistent within these limits, as can be seen in Fig. 1. Furthermore, the curvature of symmetry energy,  $K_{\text{sym}}^0$  comes out to  $-23.8$  MeV, which lies within the limits  $K_{\text{sym}}^0 \approx -107 \pm 88$  MeV obtained from the 16 new analyses [12] of neutron star observables after GW170817.

Of particular importance is the value of symmetry energy at suprasaturation densities at around  $2\rho_0$ , since the pressure around this density determines the radii of canonical neutron stars [48]. Recent studies [12] constrain the value of  $J(2\rho_0)$  to  $51 \pm 13$  MeV at 68% confidence level. In the present study, the value lies within 53.2 to 72.8 MeV, in good agreement with data extracted from heavy-ion reaction experiments.

## B. Neutron star matter

For neutron star matter under  $\beta$  equilibrium and charge neutrality conditions, we use the energy density (19) and pressure (20) with relevant changes [27–29] for the different compositions. For matter with only nucleons, the values of the maximum mass  $M_{\text{max}}$ , radius ( $R$ ), radius corresponding to the canonical star mass  $1.4M_{\odot}$  ( $R_{1.4}$ ) and the dimensionless



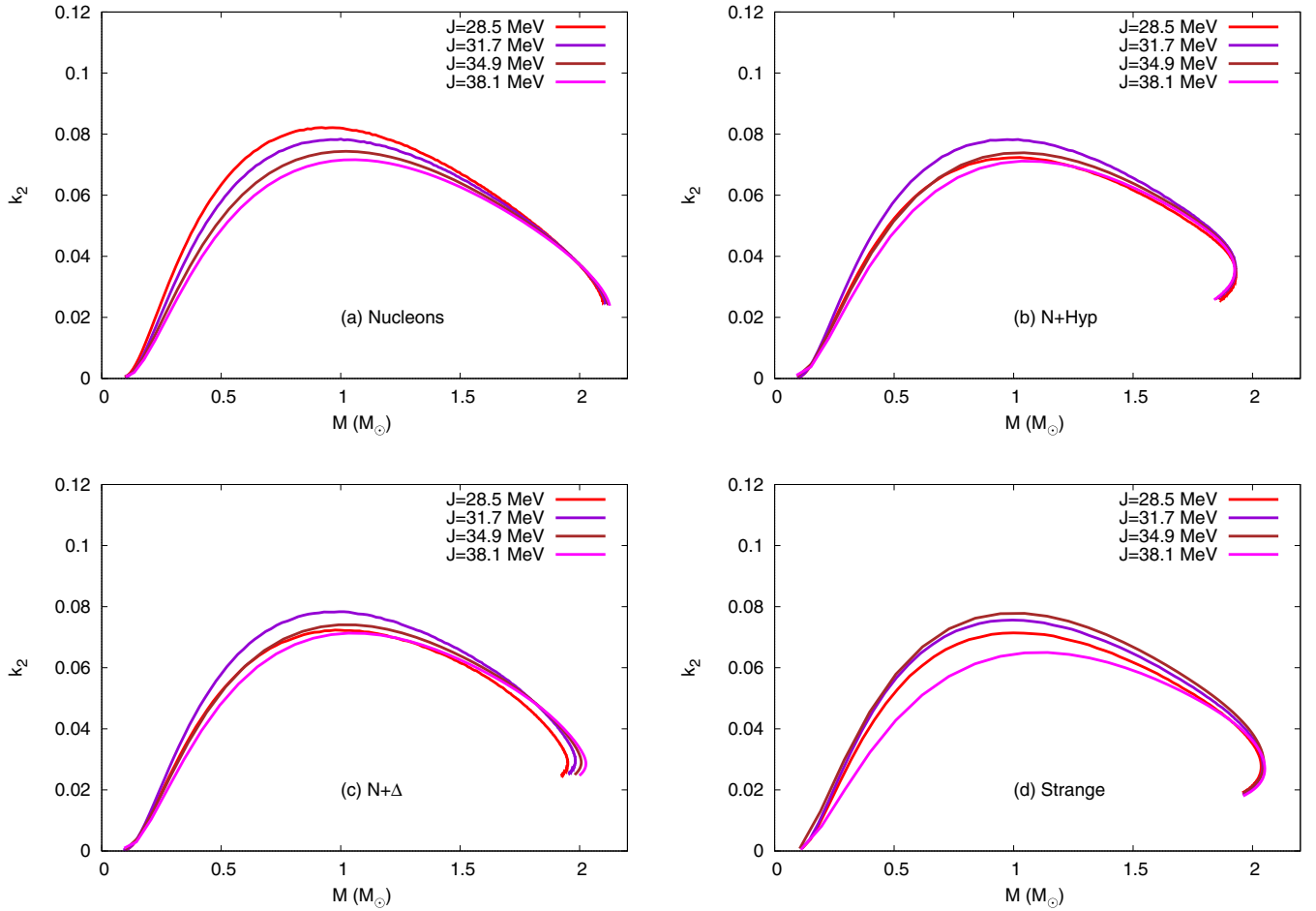


FIG. 3. Love number as a function of mass of star.

tidal deformability  $\Lambda_D$  for different  $J$  are given in Table II. We obtain a massive star with maximum mass of  $2.12 M_\odot$  and the corresponding radius varying between  $11.6 \leq R \leq 11.9$  km. The  $R_{1.4}$  value comes between  $13.6 \leq R_{1.4} \leq 14.1$  km.

For matter including nucleons and hyperons, the meson-hyperon coupling constants are fixed as follows. The hyperon couplings to the  $\omega$  meson are fixed by determining  $x_{\omega B}$  which is obtained [41,49,50] from the hyperon potentials in nuclear matter,  $U_B = -(M_B - M_B^*) + x_{\omega B} g_\omega \omega_0$  for  $B = \Lambda, \Sigma,$  and  $\Xi$  with  $U_\Lambda = -28$  MeV,  $U_\Sigma = 30$  MeV, and at  $U_\Xi = -10$  MeV. With  $m_{u,d} = 200$  MeV and  $m_s = 280$  MeV, the values for  $x_{\omega\Lambda} = 0.82541$ ,  $x_{\omega\Sigma} = 1.45353$ , and  $x_{\omega\Xi} = 0.52541$ , while we fix  $x_{\rho B} = 1$ . The values of  $M_{\max}$ ,  $R$ ,  $R_{1.4}$ , and  $\Lambda_D$  with hyperonic configuration is shown in Table III. Since the presence of hyperons significantly softens the EoS, we obtain a lower maximum mass of  $1.93 M_\odot$  while the radius varies between  $12.4 \leq R \leq 12.8$  km. Several studies have been conducted on the impact of presence of the hyperons on the mass of the neutron stars. In particular, the quark-meson-coupling model suggests [22] a mass range of  $1.9$ – $2.1 M_\odot$  with the inclusion of hyperons.

For matter with  $\Delta$  isobars [28], we fix  $x_{\omega\Delta} = 0.7$ , while the  $\Delta$  coupling to the  $\rho$  meson is fixed at  $x_{\rho\Delta} = 1$ . The mass-radius results are shown in Table IV. Here also we

observe a steady increase in the radius with increase in the stiffness of the symmetry energy. It may be noted here that the formation of  $\Delta$  isobars in neutron star matter has been a subject of intense research. A seminal work by Glendenning [51] had suggested the absence of  $\Delta$  matter in neutron stars. A recent study by Motta *et al.* [24] using the QMC model also predicted the absence of  $\Delta$  matter in neutron stars. However, a large number of studies [28,52–58] indicate the possibility of formation of  $\Delta$  isobars in neutron star matter.

We next introduce strange interactions [29] via strange meson couplings to hyperons mediated through the hidden strange mesons  $\sigma^*$  and  $\phi$  [59] which couple only to the strange quark and the hyperons of the nuclear matter. The nonstrange and strange meson couplings to the hyperons are fixed using the SU(3) flavor symmetry [29,60–64]. The results are given in Table V.

Figure 2 shows the neutron star masses as a function of their radii for four different compositions tabulated above. The variation in symmetry energy and its slope  $L$  do not have much impact on the maximum mass, with variations lying within  $0.03 M_\odot$ . However, for the  $N + \Delta$  composition the mass variation with  $J$  ranging from 28.5 MeV to 38.1 MeV is up to  $0.07 M_\odot$ , which may be attributed

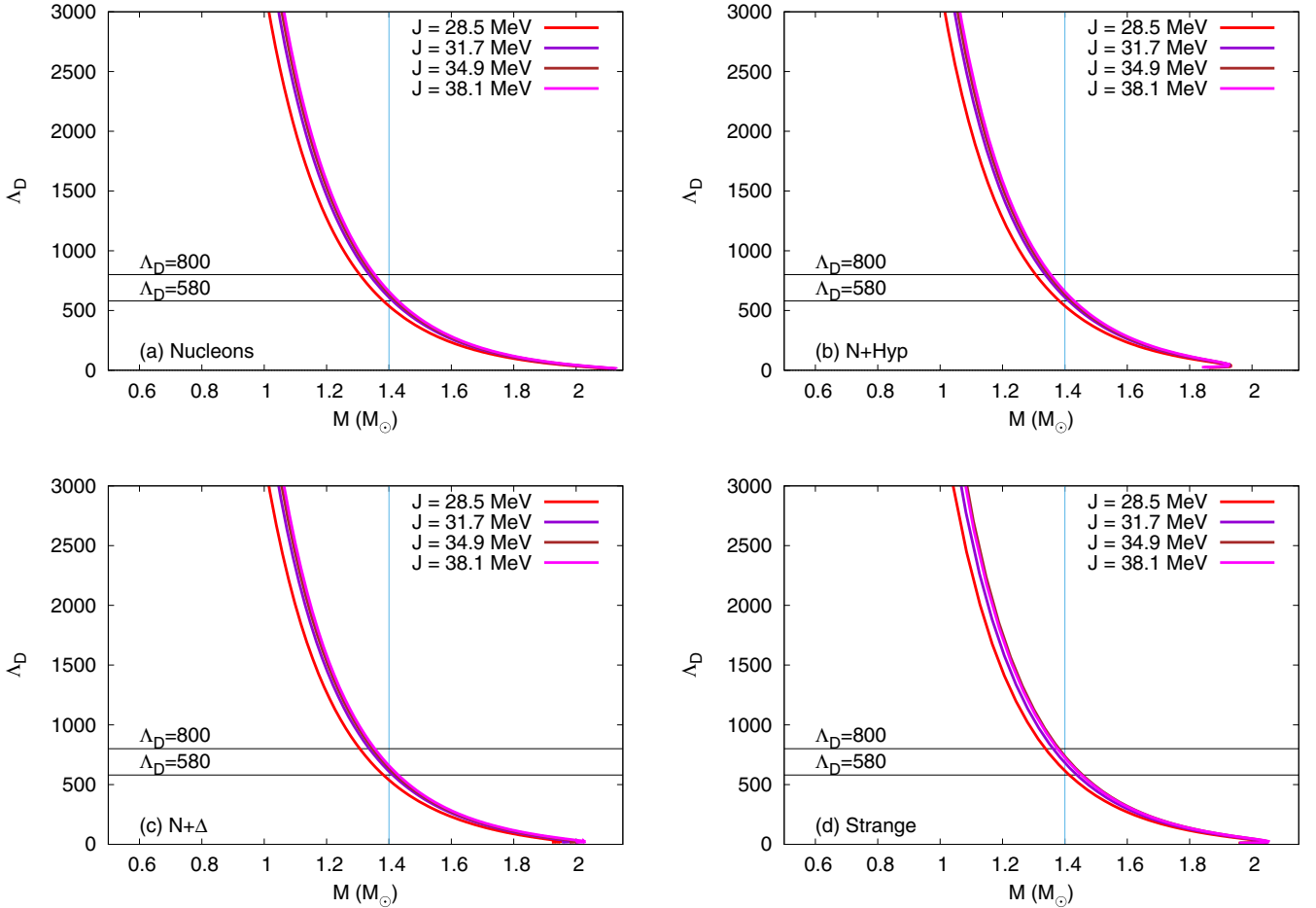


FIG. 4. Tidal deformability as a function of neutron star mass for different compositions. The vertical line indicates the canonical mass while the horizontal lines indicate earlier [30] and revised [31] upper limits of the  $\Lambda_D$ .

[28] to the increase in the  $\rho$ - $\Delta$  coupling strength with increase in  $J$ .

Over all the configurations, the maximum mass varies within  $1.93 \leq M \leq 2.12 M_\odot$  for different compositions. The mass of the pulsar PSR J0740+6620 from NICER observations has recently been updated [36,37,65] to  $2.08 \pm 0.07 M_\odot$  with the corresponding radius being  $13.7^{+2.6}_{-1.5}$  km in one study [36] and  $12.39^{+1.30}_{-0.98}$  km in another [37]. Our radius values corresponding to the maximum mass vary within 0.3–0.5 km for the chosen  $J$  values, with  $11.8 \leq R \leq 12.8$  km. This lies within the limits of the measured values of the pulsar PSR J0740+6620.

The canonical radius  $R_{1.4}$  is also sensitive to variations in the  $J$  value within 0.6 km for the different cases and lies between  $13.5 \leq R_{1.4} \leq 14.5$  km overall. The recent mass-radius estimates of the millisecond pulsar PSR J0030+0451 observed using the NICER facility [34,35] predicts a mass of  $M = 1.44^{+0.15}_{-0.14} M_\odot$  and radius  $R = 13.02^{+1.24}_{-1.06}$  km with a 68% confidence level. Our results for  $R_{1.4}$  are consistent with the predicted estimates PSR J0030+0451.

In Fig. 3 we plot the Love number  $k_2$ , which is essential for a description [66–68] of the dimensionless tidal deformability parameter  $\Lambda_D$  required to connect the gravitational wave data

with the EoS. Figure 4 shows the variation of  $\Lambda_D$  with star mass for different  $J$  with various compositions. Recently, the LIGO and Virgo collaboration has revised the limits [31] of  $\Lambda_D$  for a  $1.4 M_\odot$  star, with  $\Lambda_D = 190^{+390}_{-120}$ , which is more stringent than the earlier limit [30] of  $\Lambda_D \leq 800$ . Our results for  $\Lambda_D$  are quite consistent for the symmetry energy range of  $31.7 \pm 3.2$  MeV. However, for the stiffer  $J = 38.1$  MeV obtained from the PREX-II data, we observe higher values of  $\Lambda_D$ , indicating the tension existing between the terrestrial and astronomical observations.

The EoS developed above for both soft and stiff  $J$  satisfies most of the constraints as regards to the maximum mass and radius. However, we observe that for large  $J$ , the value of  $\Lambda_D$  is at odds with the observational data. Since the EoS at densities relevant to neutron stars is poorly understood, it would be interesting to study the behavior of two additional quantities, i.e., the speed of sound and the adiabatic index, with respect to our variation of symmetry energies.

The speed of sound, defined as  $c_s^2 = \frac{dP}{d\varepsilon}$ , is an important quantity that characterizes dense matter EoS. While the accepted range of  $c_s^2 \leq 1/3$  suggests agreement with the conformal limit, many studies [69–71] suggest that the speed of sound squared lies around or exceeds the conformal limit

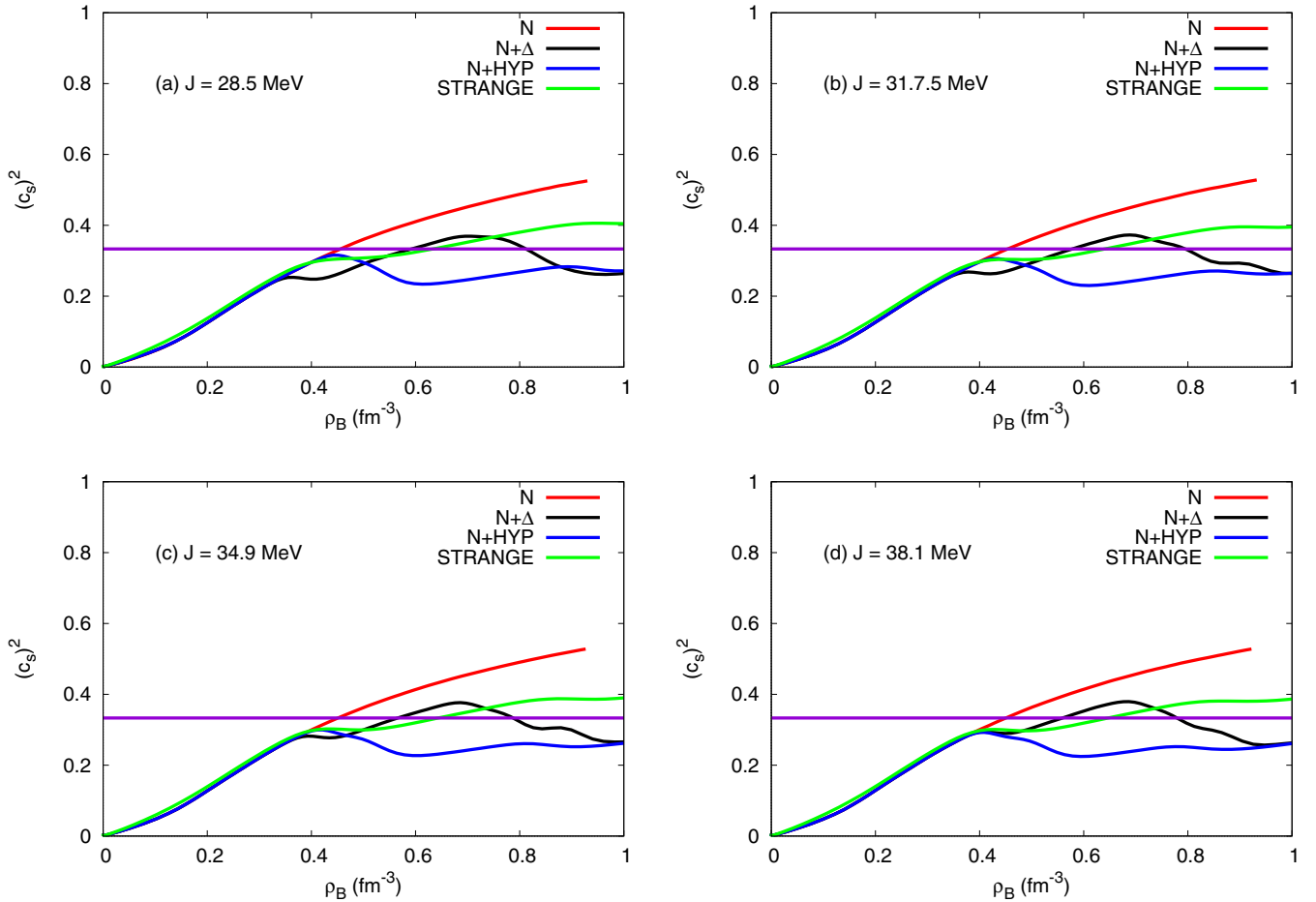


FIG. 5. The square of the speed of sound as a function of density for various compositions at different  $J$ . The horizontal line indicates the conformal limit  $c_s^2 = 1/3$ .

$c_s^2 \leq 1/3$ . Recently, Annala *et al.* [72] applied a new ‘speed-of-sound’ interpolation method to suggest that agreement with the conformal limit in massive neutron stars can predict sizable quark-matter cores. In the present work, it is observed that all four compositions have a speed of sound near or below the conformal limit of  $c_s^2 \leq 1/3$ . Since the present study involves hyperons [73] as well as  $\Delta$ ’s, the change in the degrees of freedom results in dips and kinks in  $c_s^2$ . Such behavior is observed in Fig. 5 which shows the variation in  $c_s^2$  with density.

Another significant thermodynamic quantity [74–78] related to the EoS is the adiabatic index  $\Gamma$ , that is sensitive to changes in the composition of matter. The adiabatic index can be used [79] to impose constraints on realistic equations of state so as to obtain stable configurations of neutron stars. For most of the EoS’s of neutron star matter,  $\Gamma$  varies from 2 to 4. Since we have chosen four possible compositions at different  $J$ , we observe that the variation of  $\Gamma$  for our EoS’s at different  $J$  (including the stiffest 38.1 MeV) satisfies the range of 2 to 4. Further, the dips and kinks in the variation of  $\Gamma$  is due to the appearance of different baryon species at different densities [78]. This is shown in Fig. 6 for different cases of  $J$ .

## V. CONCLUSION

In the present work we have studied the effect of variation of symmetry energy on the observational properties of neutron stars such as the mass, radius and tidal deformability using a relativistic quark model. The contrasting values of  $J$  due to the astrophysical and terrestrial observations has created new challenges to constrain the dense matter EoS. We find that a stiff symmetry is able to satisfy the neutron star mass and radius constraints from NICER observations but unable to satisfy the stringent constraints on tidal deformability parameter. We also study the behavior of the speed of sound and adiabatic index and find that all our EoS at different  $J$  and different compositions satisfy the conformal limits.

## ACKNOWLEDGMENTS

P.K.P. acknowledges the financial assistance from DST(FIST), India, for the Project No. SR/FST/PS-II/2017/22. S.K. acknowledges support from DST, Government of India, via DST-INSPIRE Fellowship Regd. No. IF160976.



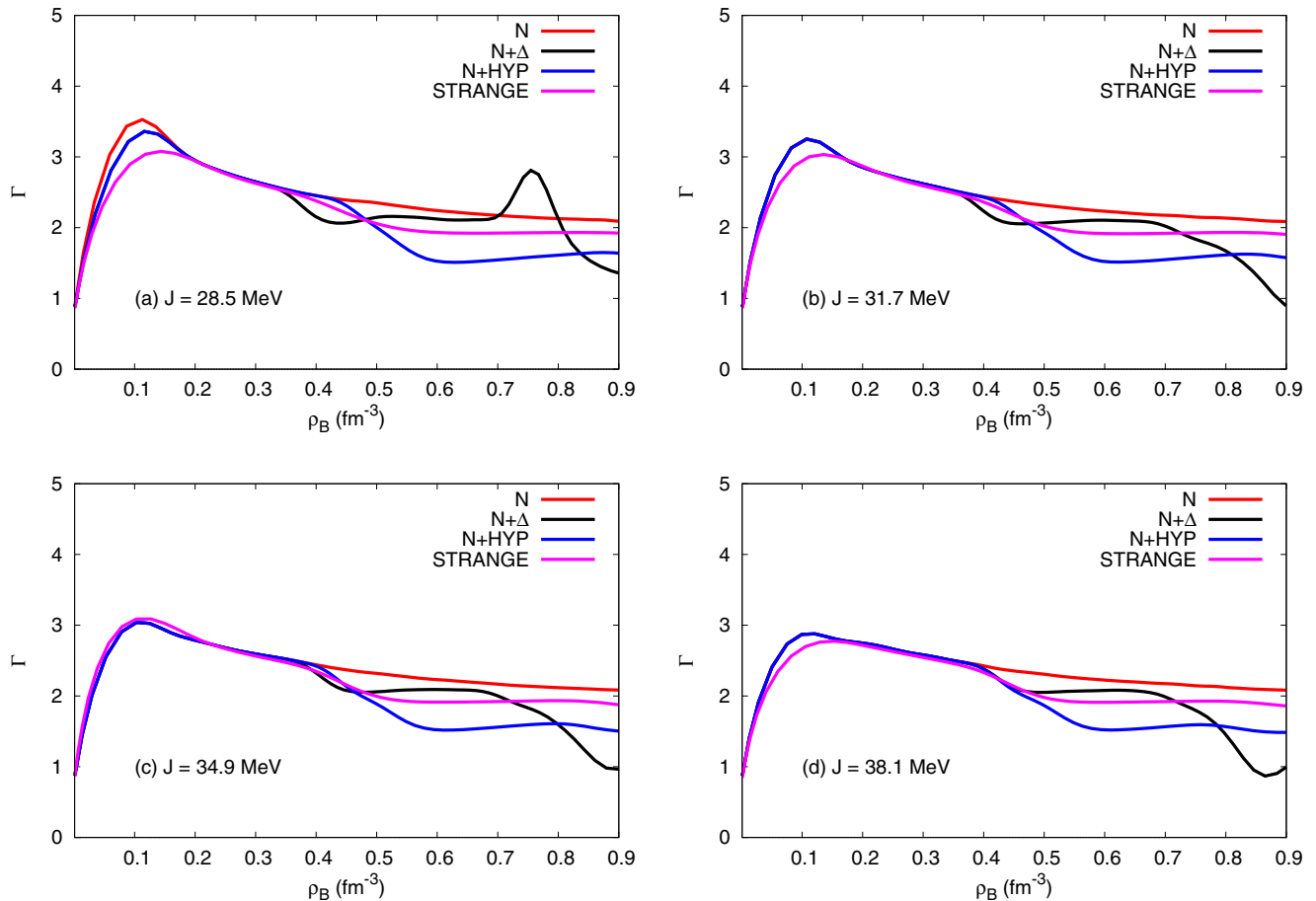


FIG. 6. The adiabatic index as a function of density for different compositions.

- [1] D. Adhikari *et al.*, *Phys. Rev. Lett.* **126**, 172502 (2021).
- [2] B. T. Reed, F. J. Fattoyev, C. J. Horowitz, and J. Piekarewicz, *Phys. Rev. Lett.* **126**, 172503 (2021).
- [3] Z. Zhang and L.-W. Chen, *Phys. Lett. B* **726**, 234 (2013).
- [4] K. Hebeler, J. Lattimer, C. Pethick, and A. Schwenk, *Astrophys. J.* **773**, 11 (2013).
- [5] C. Drischler, R. J. Furnstahl, J. A. Melendez, and D. R. Phillips, *Phys. Rev. Lett.* **125**, 202702 (2020).
- [6] G. Hagen *et al.*, *Nat. Phys.* **12**, 186 (2015).
- [7] L.-W. Chen, C. M. Ko, B.-A. Li, and J. Xu, *Phys. Rev. C* **82**, 024321 (2010).
- [8] A. W. Steiner and S. Gandol, *Phys. Rev. Lett.* **108**, 081102 (2012).
- [9] S. Gandol, J. Carlson, S. Reddy, A. Steiner, and R. Wiringa, *Eur. Phys. J. A* **50**, 10 (2014).
- [10] B. A. Li and X. Han, *Phys. Lett. B* **727**, 276 (2013).
- [11] M. Oertel, M. Hempel, T. Klähn, and S. Typel, *Rev. Mod. Phys.* **89**, 015007 (2017).
- [12] B.-A. Li, B.-J. Cai, W.-J. Xie, and N.-B. Zhang, *Universe* **7**, 182 (2021).
- [13] J. Estee *et al.* ( $S\pi$  RIT Collaboration), *Phys. Rev. Lett.* **126**, 162701 (2021).
- [14] J. Piekarewicz, *Phys. Rev. C* **104**, 024329 (2021).
- [15] P. A. M. Guichon, *Phys. Lett. B* **200**, 235 (1988).
- [16] T. Frederico, B. V. Carlson, R. A. Rego, and M. S. Hussein, *J. Phys. G* **15**, 297 (1989).
- [17] K. Saito and A. W. Thomas, *Phys. Lett. B* **327**, 9 (1994); **335**, 17 (1994); **363**, 157 (1995); *Phys. Rev. C* **52**, 2789 (1995).
- [18] K. Saito, K. Tsushima, and A. W. Thomas, *Nucl. Phys. A* **609**, 339 (1996); *Phys. Rev. C* **55**, 2637 (1997); *Phys. Lett. B* **406**, 287 (1997).
- [19] P. G. Blunden and G. A. Miller, *Phys. Rev. C* **54**, 359 (1996); H. Shen and H. Toki, *ibid.* **61**, 045205 (2000); P. K. Panda, R. Sahu, and C. Das, *ibid.* **60**, 038801 (1999); P. K. Panda, M. E. Bracco, M. Chiapparini, E. Conte, and G. Krein, *ibid.* **65**, 065206 (2002); P. K. Panda and F. L. Braghin, *ibid.* **66**, 055207 (2002).
- [20] P. K. Panda, A. Mishra, J. M. Eisenberg, and W. Greiner, *Phys. Rev. C* **56**, 3134 (1997); I. Zakout and H. R. Jaqaman, *ibid.* **59**, 962 (1999).
- [21] P. A. M. Guichon, J. R. Stone, and A. W. Thomas, *Prog. Part. Nucl. Phys.* **100**, 262 (2018).
- [22] J. R. Stone, P. A. M. Guichon, H. H. Matevosyan, and A. W. Thomas, *Nucl. Phys. A* **792**, 341 (2007).
- [23] T. F. Motta, A. M. Kalaitzis, S. Antić, P. A. M. Guichon, J. R. Stone, and A. W. Thomas, *Astrophys. J.* **878**, 159 (2019).
- [24] T. F. Motta, A. W. Thomas, and P. A. M. Guichon, *Phys. Lett. B* **802**, 135266 (2020).

- [25] N. Barik, R. N. Mishra, D. K. Mohanty, P. K. Panda, and T. Frederico, *Phys. Rev. C* **88**, 015206 (2013).
- [26] R. N. Mishra, H. S. Sahoo, P. K. Panda, N. Barik, and T. Frederico, *Phys. Rev. C* **92**, 045203 (2015).
- [27] R. N. Mishra, H. S. Sahoo, P. K. Panda, N. Barik, and T. Frederico, *Phys. Rev. C* **94**, 035805 (2016).
- [28] H. S. Sahoo, G. Mitra, R. N. Mishra, P. K. Panda, and B. A. Li, *Phys. Rev. C* **98**, 045801 (2018).
- [29] H. S. Sahoo, R. N. Mishra, D. K. Mohanty, P. K. Panda, and N. Barik, *Phys. Rev. C* **99**, 055803 (2019).
- [30] B. P. Abbott *et al.*, *Phys. Rev. Lett.* **119**, 161101 (2017).
- [31] B. P. Abbott *et al.*, *Phys. Rev. Lett.* **121**, 161101 (2018).
- [32] B. P. Abbott *et al.*, *Astrophys. J. Lett.* **892**, L3 (2020).
- [33] H. T. Cromartie *et al.*, *Nature Astron.* **4**, 72 (2019).
- [34] M. C. Miller *et al.*, *Astrophys. J. Lett.* **887**, L24 (2019).
- [35] T. E. Riley *et al.*, *Astrophys. J. Lett.* **887**, L21 (2019).
- [36] M. C. Miller *et al.*, *Astrophys. J. Lett.* **918**, L28 (2021).
- [37] T. E. Riley *et al.*, *Astrophys. J. Lett.* **918**, L27 (2021).
- [38] X. Xing, J. Hu, and H. Shen, *Phys. Rev. C* **95**, 054310 (2017).
- [39] Z.-Y. Zhu, E.-P. Zhou, and A. Li, *Astrophys. J.* **862**, 98 (2018).
- [40] A. Li, Z.-Y. Zhu *et al.*, *J. High Energy Astrophys.* **28**, 19 (2020).
- [41] P. K. Panda, D. P. Menezes, and C. Providenci, *Phys. Rev. C* **69**, 025207 (2004).
- [42] J. R. Oppenheimer and G. M. Volkoff, *Phys. Rev.* **55**, 374 (1939).
- [43] R. C. Tolman, *Proc. Nat. Acad. Sci. USA* **20**, 169 (1934).
- [44] J. M. Lattimer and M. Prakash, *Phys. Rep.* **621**, 127 (2016).
- [45] G. Baym, C. Pethick, and P. Sutherland, *Astrophys. J.* **170**, 299 (1971).
- [46] R. Pohl *et al.*, *Nature (Lond.)* **466**, 213 (2010).
- [47] B. Biswas, *Astrophys. J.* **921**, 63 (2021).
- [48] J. M. Lattimer and M. Prakash, *Astrophys. J.* **550**, 426 (2001).
- [49] P. K. Panda, C. Providenci, and D. P. Menezes, *Phys. Rev. C* **82**, 045801 (2010).
- [50] P. K. Panda, A. M. S. Santos, D. P. Menezes, and C. Providenci, *Phys. Rev. C* **85**, 055802 (2012).
- [51] N. K. Glendenning, *Astrophys. J.* **293**, 470 (1985).
- [52] A. Drago, A. Lavagno, G. Pagliara, and D. Pigato, *Phys. Rev. C* **90**, 065809 (2014).
- [53] A. Drago, A. Lavagno, and G. Pagliara, *Phys. Rev. D* **89**, 043014 (2014).
- [54] B.-J. Cai, F. J. Fattoyev, B. A. Li, and W. G. Newton, *Phys. Rev. C* **92**, 015802 (2015).
- [55] A. Drago, A. Lavagno, G. Pagliara, and D. Pigato, *Eur. Phys. J. A* **52**, 40 (2016).
- [56] Z.-Y. Zhu, A. Li, J.-N. Hu, and H. Sagawa, *Phys. Rev. C* **94**, 045803 (2016).
- [57] E. E. Kolomeitsev, K. A. Maslov, and D. N. Voskresensky, *Nucl. Phys. A* **961**, 106 (2017).
- [58] J. J. Li, A. Sedrakian, and F. Weber, *Phys. Lett. B* **783**, 234 (2018).
- [59] J. Beringer *et al.* (Particle Data Group), *Phys. Rev. D* **86**, 010001 (2012).
- [60] T. Miyatsu, M. K. Cheoun, and K. Saito, *Phys. Rev. C* **88**, 015802 (2013).
- [61] T. A. Rijken, M. M. Nagels, and Y. Yamamoto, *Prog. Theor. Phys. Suppl.* **185**, 14 (2010).
- [62] J. J. de Swart, *Rev. Mod. Phys.* **35**, 916 (1963); **37**, 326(E) (1965).
- [63] T. A. Rijken, V. G. J. Stoks, and Y. Yamamoto, *Phys. Rev. C* **59**, 21 (1999).
- [64] S. Weissenborn, D. Chatterjee, and J. Schaffner-Bielich, *Phys. Rev. C* **85**, 065802 (2012); *Nucl. Phys. A* **881**, 62 (2012).
- [65] E. Fonseca *et al.*, *Astrophys. J. Lett.* **915**, L12 (2021).
- [66] E. E. Flanagan and T. Hinderer, *Phys. Rev. D* **77**, 021502(R) (2008).
- [67] T. Hinderer, *Astrophys. J.* **677**, 1216 (2008).
- [68] S. Postnikov, M. Prakash, and J. M. Lattimer, *Phys. Rev. D* **82**, 024016 (2010).
- [69] P. Bedaque and A. W. Steiner, *Phys. Rev. Lett.* **114**, 031103 (2015).
- [70] I. Tews, J. Carlson, S. Gandolfi, and S. Reddy, *Astrophys. J.* **860**, 149 (2018).
- [71] A. Cherman, T. D. Cohen, and A. Nellore, *Phys. Rev. D* **80**, 066003 (2009).
- [72] E. Annala *et al.*, *Nat. Phys.* **16**, 907 (2020).
- [73] T. F. Motta, P. A. M. Guichon, and A. W. Thomas, *Nucl. Phys. A* **1009**, 122157 (2021).
- [74] A. Akmal, V. R. Pandharipande, and D. G. Ravenhall, *Phys. Rev. C* **58**, 1804 (1998).
- [75] P. Haensel, K. P. Levenfish, and D. G. Yakovlev, *Astron. Astrophys.* **394**, 213 (2002).
- [76] N. Chamel and P. Haensel, *Living Rev. Relativ.* **11**, 10 (2008).
- [77] R. H. Casali and D. P. Menezes, *Braz. J. Phys.* **40**, 166 (2010).
- [78] J. R. Stone, V. Dexheimer, P. A. M. Guichon, A. W. Thomas, and S. Typel, *Mon. Not. Roy. Astron. Soc.* **502**, 3476 (2021).
- [79] Ch. C. Moustakidis, *Gen. Relativ. Gravit.* **49**, 68 (2017).